Original

Stuepp, C.A.; Mendis, C.L.; Mohedano, M.; Szakacs, G.; Gensch, F.;
Mueller, S.; Feyerabend, F.; Hortza, D.; Fredel, M.C.; Hort, N.:

Powder Metallurgical Synthesis of Biodegradable Mg-Hydroxyapatite Composites for Biomedical Applications

Materials Science Forum, Light Metals Technology 2015 (2015)
Trans Tech Publications

DOI: 10.4028/www.scientific.net/MSF.828-829.165

Materials Science Forum
ISSN: 1662-9752, Vols. 828-829, pp 165-171
doi:10.4028/www.scientific.net/MSF.828-829.165

Submitted: 2015-01-29
Revised: 2015-05-13
Accepted: 2015-05-14
Online: 2015-08-26

Powder Metallurgical Synthesis of Biodegradable Mg-hydroxyapatite Composites for Biomedical applications

CÉSAR Augusto Stüpp[1,2,a] *, CHAMINI Lakshi Mendis[1,b], MARTA Mohedano[1,c] GÁBOR Szakács[1,d], FELIX Gensch[3,e], SÖREN Müller[3,f], FRANK Feyerabend[1,g], DACHAMIR Hotza[2,h], MARCIO Celso Fredel[2,i] and NORBERT Hort[1,j]

[1]Institute of Materials Research, Helmholtz-Zentrum Geesthacht, Geesthacht, Germany

[2] Federal University of Santa Catarina, Florianópolis, Santa Catarina, Brazil

[3]Forschungszentrum Strangpressen, TU Berlin, Gustav-Meyer-Allee 25, 13355 Berlin, Germany

[a]cesar.stupp@gmail.com, [b]chamini.mendis@hzg.de, [c]marta.mohedano@hzg.de
[d]gabor.szakacs@hzg.de, [e]felix.gensch@fzs-berlin.de, [f]soeren.mueller@tu-berlin.de,
[g]frank.feyerabend@hzg.de, [h]dhotza@gmail.com, [i]m.fredel@ufsc.br, [j]norbert.hort@hzg.de*

Keywords: Mg-MMC, hydroxyapatite, corrosion behaviour, mechanical properties.

Abstract: Biodegradable Mg alloys are a new class of temporary implant materials for musculo-skeletal surgery. Recent studies show that Mg-based alloys can be biocompatible and there is a high demand to design Mg alloys with adjustable corrosion rates and suitable mechanical properties. An approach to solving this challenge might be the use of Mg metal matrix composites (Mg-MMC). In this study, a Mg-MMC composed of ZK60 was investigated as the base material and hydroxyapatite (HA) particles were added for tailoring its properties. The composite was produced by high-energy ball milling followed by hot extrusion. The HA particles were homogeneously distributed in the ZK60 matrix after ball milling and the composite was consolidated by hot extrusion. This work presents the influence of different amounts of HA on corrosion behaviour and mechanical properties of the composite. Corrosion properties were evaluated by immersion and electrochemical measurements in physiological media at 37 °C. A slight improvement in the corrosion resistance was observed for Mg-MMC most likely due to the presence of more stable corrosion products. Compression tests were used to measure the mechanical properties. Under compression, samples showed a slight increase in the compressive yield strength with the addition of HA, while the ultimate strength did not change significantly.

Introduction

One of the most important advantages of temporary implants based on biodegradable materials is that a second surgery for the removal of these is not required, supressing the possibility of errors during implant retrieval or revision [1]. The biodegradable implants also return the affected joint very close to its original condition [2]. Research on Mg alloys as biodegradable implant has grown in the last decade [3]. This interest is largely fuelled by the non-toxicity, mechanical properties close to those of bone, as well as degradability and biocompatibility of Mg alloys [4, 5]. Mg is a common constituent in the human body, where at least half of it is stored in bone tissues [1] and it can be absorbed, consumed or excreted within a period of time [6].

The loss of mechanical integrity before the surrounded tissue heals can occur due to rapid corrosion of Mg [7]. Studies show approaches to solve the high degradation rates of Mg by systematically controlling the rate of degradation by alloy design and appropriate thermo-mechanical processing [8, 9, 10]. Mg-MMC containing ceramic particles such as SiC are investigated to enhance the yield strength for structural applications [11]. However, the addition of SiC results in reduced corrosion resistance compared with the base alloy [12]. Recently, it was reported that the addition of hydroxyapatite (HA) enhanced the corrosion resistance of Mg alloys

but did not deteriorate the mechanical properties of the composite [2, 10]. In previous investigations corrosion behaviour was measured in simulated body fluid (mixture of salts similar to that in physiological environment) [2] and in NaCl and cell culture [10] solution. It has been established that such solutions do not essentially mimic the physiological conditions and there is no direct correlation between corrosion in NaCl solutions and solutions that mimic physiological environments [13].

In this investigation composites with HA additions of 7.5 wt.% (4.5 vol.%), 10 wt.% (6 vol.%) and 20 wt.% (13 vol.%) and the ZK60 (Mg-6Zn-0.6Zr (wt.%)) alloy with no HA addition as control were fabricated. Effect of HA on the microstructure of the extruded composites is reported along with detailed characterization of compressive mechanical properties and corrosion behaviour. For easier understanding, the convention ZK60, ZK60-7.5, ZK60-10 and ZK60-20 is adopted for the composites with 0, 7.5, 10 and 20 wt.%, respectively.

Experimental procedure

Mg chips were prepared by machining ingots of ZK60 alloy. The HA (particle size <42 μm) was purchased from Alfa Aesar GmbH, Germany. The ZK60 chips and HA particles were mixed in appropriate concentrations, and milled in the ball mill for 7 h at 250 rpm with a ball to powder ratio (BPR) of 20:1. The powder was then hot extruded at 270 ºC, with an extrusion ratio of 1:10 and a speed of 9 mm/s to consolidate the material. Specimens were embedded in epoxy, ground with SiC papers with a grit size from 500 to 2500 mesh and polished with water-free 0.5 μm colloidal silica suspension for optical microscopy observations. The specimens were etched in a solution of ethanol (70%), distilled water (20%), acetic acid (5%) and 8-9 g of picric acid. The optical microscopy observations were conducted on Reichert-Jung MeF3 optical microscope.

Samples for compression tests were prepared from the extruded bars by machining with 9.5 mm diameter and 17 mm length, according to DIN 50106 [14]. A Zwick 050 testing machine with a strain gauge was used for compression tests, at room temperature at an initial strain rate of 10^{-3} s^{-1}. Five specimens from each composite were tested to allow sample scatter.

Electrochemical experiments were performed using two different solutions at 37 ^{o}C using an ACM Gill AC computer controlled potentiostat to evaluate the corrosion behaviour of the specimens. A corrosion cell (333 ml) with a three-electrode set-up consisted of a saturated Ag/AgCl reference electrode, a platinum (mesh) counter electrode, and the specimen as working electrode were used. Potentiodynamic polarization curves were carried out starting at –150 mV relative to OCP (measured after 30 min of immersion) at a sweep rate of 0.2 mV s^{-1} until the anodic branch reached a final current density of 0.01 mA cm^{-2}. The experiments were conducted in Hank's solution (pH 7.8) and to reproduce physiological conditions more closely the electro-chemical testing in DMEM (Dulbecco's Modified Eagle Media) with Glutamax containing 10% of fetal bovine serum (FBS) was performed. From the cathodic branch of the polarization curve, the corrosion rate was determined using the Tafel slope. Immersion tests to investigate the weight loss (sample size: diameter 8.5 mm and thickness 3 mm) were conducted according to ISO 10993-5 [15]. The specimens were autoclaved at 121 ^{o}C for 20 min for sterilization prior to immersion in 3 ml of DMEM + 10 vol.% FBS for 72h at 37 ^{o}C with a controlled test environment (5% CO_2, 20% O_2 and 95% relative humidity). Samples were cleaned with chromic acid (180 g/L) to remove corrosion products and dried for 24 h at 50 ºC. Specimens were weighed prior to immersion tests and after the removal of the corrosion products, to determine the corrosion rate.

Results and discussion

The optical microstructures showing the grain size of the alloy and composites and HA distribution the composites are shown in Fig. 1. In all samples there is a duplex distribution of the grain sizes with the microstructure mainly composed of fine grains with few regions containing coarse grains. The ZK60, Fig. 1 (a) contain coarse grained regions with a grain size of ~40 μm and regions of fine grains of approximately 1 μm due to oxide particles preventing grain growth. The dark particles

forming in stringers parallel to extrusion direction, Fig. 1 (a) are oxide particles from the surface of the ZK60 chips. The increase in HA content, Fig. 1 (b-d) show an increase in the volume of dark stringers due to the increased volume of HA. With the addition of HA, the number of regions with coarse grains decrease and the fine grain regions become more prevalent and ZK60-20, Fig. 1 (d), contained mainly fine grained regions with grain size not resolvable using optical microscopy. In the ZK60-20 alloy the coarse grained regions contained a grain size of ~15 µm. The microstructures of the ZK60-20 alloy may be compared with the AZ91-20HA reported by Witte et al [10] but the ZK60-20 contained a duplex grain structure that was not observed with the AZ91 alloy. Grain refinement in the presence of reinforcements has been observed previously in AZ91/SiC composites [16] similar to that observed here. The addition of HA decreased the grain size significantly thus providing surfaces where recrystallization can occur, possibly through particle stimulated nucleation or the HA particles prevent grain growth. The determination of the exact mechanism that control the refined grain size is beyond the scope of this contribution

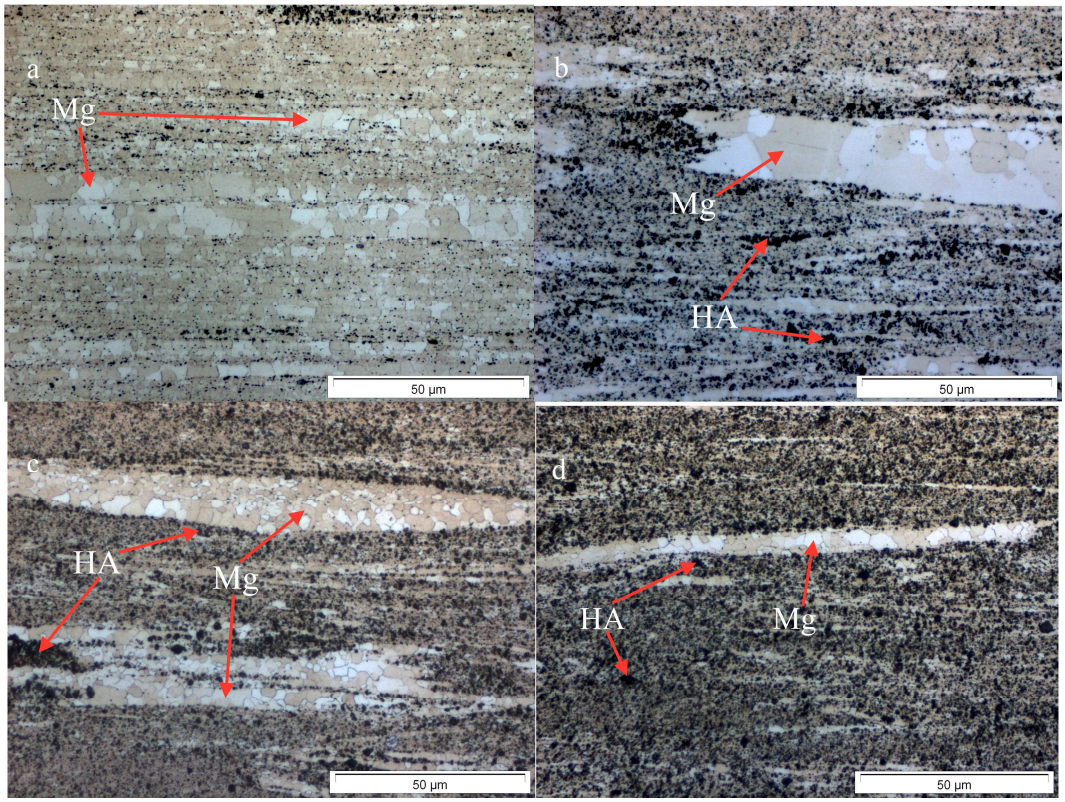

Fig. 1. Optical micrographs of the ZK60 (a) and the composites ZK60-7.5 (b), ZK60-10 (c) and ZK60-20 (d).

The compression stress-strain curves are shown in Fig. 2 and the pertinent features are summarized in Table 1. The compression stress-strain curves show that the yield strength and the ultimate strength increase with increased HA content similar to the observations in [2], while the elongation to failure decreased. The increase in yield strength with HA additions was approximately 60 MPa for ZK60-20, while the UCS increased by approximately 14%. Elongation to failure decreased by ~46% with the addition of 20 wt.% HA still showing a ductile behaviour.

Table 1. Room temperature compressive mechanical properties for the ball milled and extruded ZK60 alloy, ZK60-7.5, ZK60-10 and ZK60-20.

Material	0.2%CYS [MPa]	UCS [MPa]	Elongation [%]
ZK60	277 ± 22	485 ± 35	9.5 ± 1.0
ZK60-7.5	351 ± 19	520 ± 26	7.2 ± 0.6
ZK60-10	341 ± 20	529 ± 13	6.6 ± 0.4
ZK60-20	356 ± 54	554 ± 20	5.1 ± 0.4

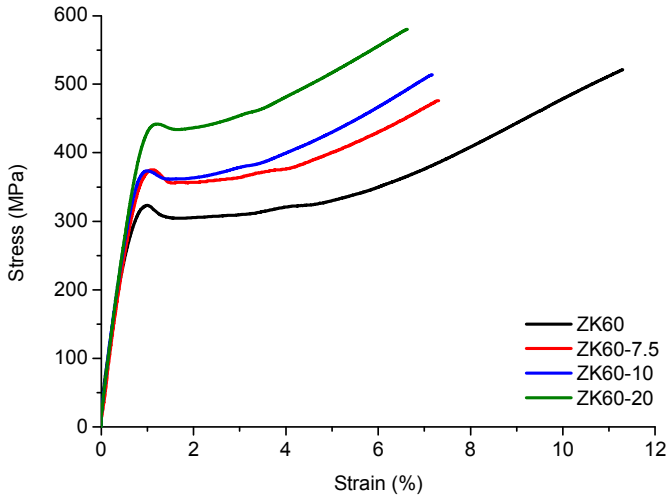

Fig. 2. The nominal stress-strain curves for the compression of the as-extruded ZK60 alloy and HA containing composites.

The derived electrochemical parameters from the potentio-dynamic polarization are listed in Table 2, while the curves are shown in Fig. 3. In Hank's solution, the addition of HA brought the E_{corr} to less nobler potentials up to 10% addition and to slightly nobler values for ZK60-20. The i_{corr} did not follow a trend and increased with 7.5 and 10% HA addition but decreased for ZK60-20. All the specimens showed a passive range in Hank's solution with E_{pitt} at approximately -1350 to -1300 mV. This behaviour is related to the oxide layer on top of the alloy (SEM results not shown here), which developed during autoclaving. The differences in these values are attributed to the heterogeneity of this layer. When the composites were not autoclaved (results not shown here) such behaviour was not observed.

Table 2. Electrochemical parameters derived from potentiodynamic polarization curves.

Materials	Hank's solution			DMEM + 10 vol.% FBS	
	E_{corr} [mV]	i_{corr} [µA/cm^2]	E_{pitt}-E_{corr} [mV]	E_{corr} [mV]	i_{corr} [µA/cm^2]
ZK60	-1405.50	0.0035	81.90	-1506.50	0.0847
ZK60-7.5	-1455.90	0.0062	98.00	-1470.40	0.0453
ZK60-10	-1437.40	0.0036	112.50	-1469.20	0.0643
ZK60-20	-1399.10	0.0017	92.60	-1485.50	0.0453

The potentio-dynamic polarization curves in DMEM did not show a passive range. That suggests that there is no visible protective effect due the autoclaved oxide layer when the specimens are

exposed to DMEM solution. With HA addition a slightly lower i_{corr} and slightly nobler E_{corr} are reported. The differences in the results, which did not follow a trend with the addition of HA, are likely to be associated with the oxide layer that formed during autoclaving.

The corrosion rates measured with immersion tests in DMEM + FBS are shown in Table 3. Up to 7.5 wt.% of HA addition an increase in the corrosion rate was observed, which began to decrease with more than 10 wt.%, reaching the lowest corrosion rate, for the ZK60-20 composite, which can also be due to the fact that there is less Mg to corrode at higher HA additions. This is similar to previous observations [17], but is contrasted with [18]. Fig. 3 shows the samples after immersion and corrosion products removal with chromic acid. There is severe localized corrosion in all the samples. The area fraction associated with the localized corrosion seems to decrease with the addition of up to 20 wt.% HA. The reasons behind the localized corrosion are not yet clear. It is proposed to be due to the rupture of the very thin oxide layer that forms during autoclaving or due to inhomogeneous nature of this layer.

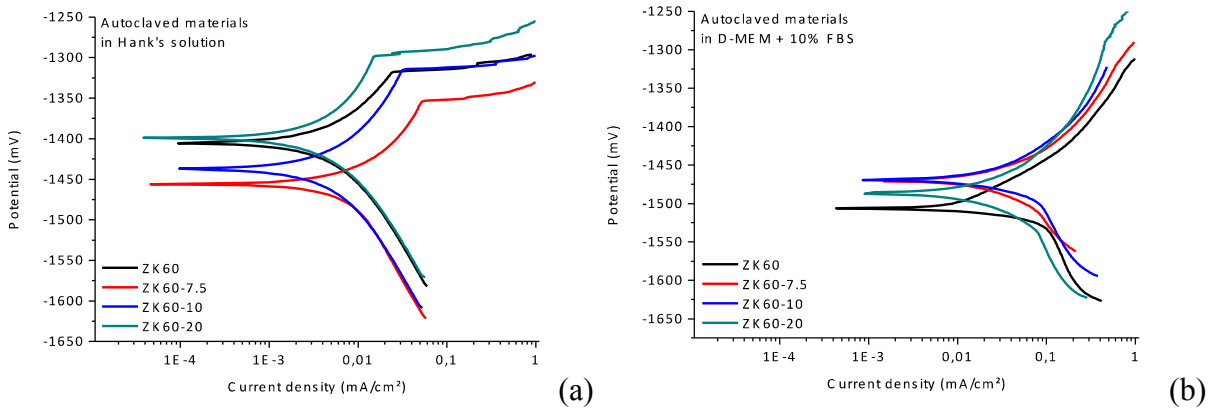

Fig. 3. Potentio-dynamic polarisation curves for the autoclaved ZK60 with 0-20% HA in (a) hank solution and (b) DMEM+10%FBS.

Table 3. The corrosion rates for all the composites after immersion for 72 h in DMEM + 10 vol.% FBS solution.

Material	Corrosion rate [mm/year]
ZK60	0.50 ± 0.16
ZK60-7.5	0.54 ± 0.09
ZK60-10	0.47 ± 0.14
ZK60-20	0.41 ± 0.10

Conclusions

ZK60 magnesium composites with different amounts of hydroxyapatite were successfully fabricated by ball milling and hot extrusion. The grain size of the composite decreased substantially, it is assumed this decrease in grain size was mainly due to addition of HA The composite shows an increase in the compressive yield strength and ultimate compressive strength while the elongation decreased by adding HA. Immersion tests showed that the corrosion rate decreases with more than 10 wt.% of HA, while it increases slightly with 7.5 wt.% of HA. It was also shown that the corrosion is general with some localized pitting corrosion. Potentiodynamic polarization curves in Hank's solution showed the same trend, except that for ZK60-7.5, there is a small increase in

current density compared with ZK60, and it only decreases when adding 20 wt.%. In DMEM + 10 vol.% of FBS, the difference is clearer. By adding any amount of HA, corrosion density decreases, and potentials are nobler, indicating an improvement in the corrosion resistance of the MMCs developed.

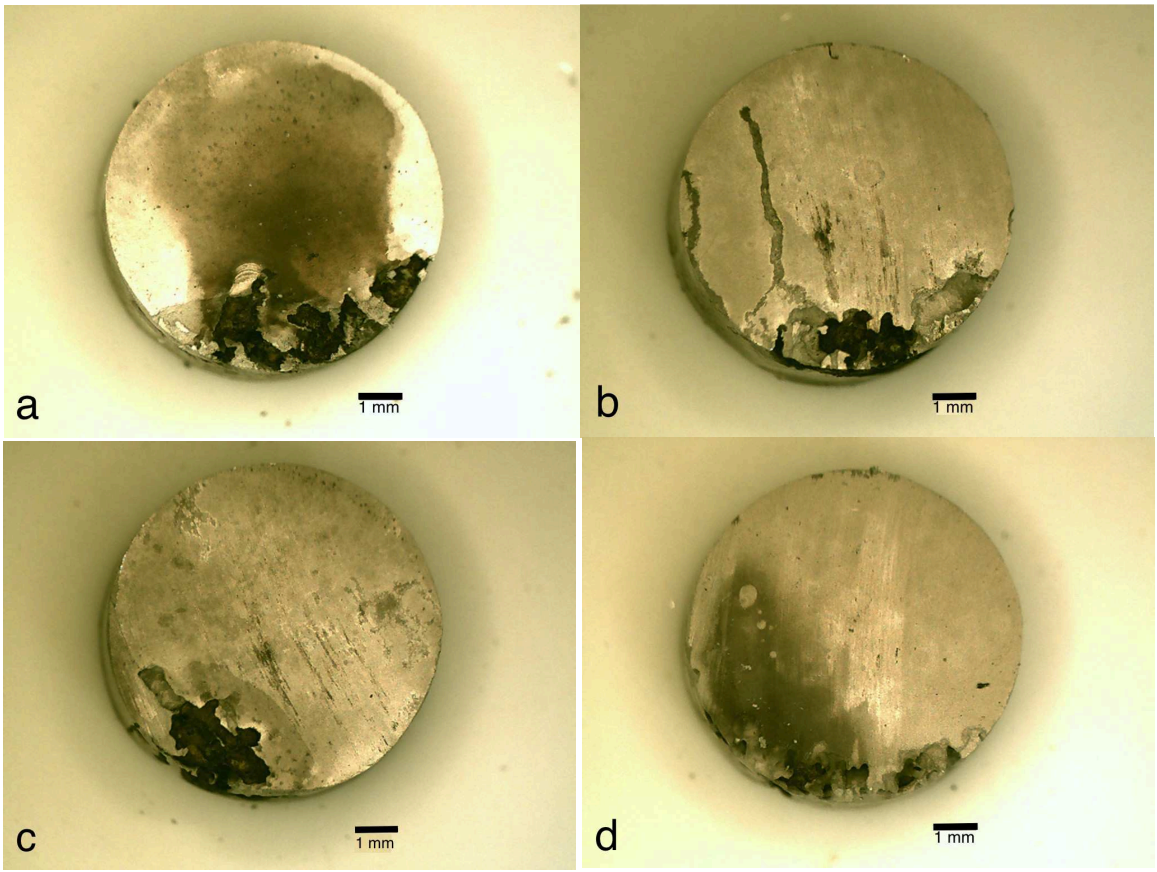

Fig. 4. Samples after 72 h immersion in DMEM + 10 vol.% FBS. From (a) to (d): ZK60, ZK60-7.5, ZK60-10, ZK60-20.

Acknowledgements

C.S. acknowledges the project BRAGECRIM for the provision of financial support in form of a scholarship provided by CAPES. M.M acknowledges Alexander von Humboldt Foundation for the provision of financial support through the post-doctoral fellowship program.

References

[1] Edited by F. Czerwinski, Magnesium alloys – design, processing and properties, InTech: Rijeka, Croatia (2011).

[2] A. Feng and Y. Han, The microstructure, mechanical and corrosion properties of calcium polyphosphate reinforced ZK60A magnesium alloy composites, Journal of Alloys and Compounds 504 (2010) 585-593.

[3] Z. Li, Mg/Hydroxyapatite composites for potential bio-medical applications, PhD thesis, Brunel University, London, 2010.

[4] N.T. Kirkland and N. Birbilis, Magnesium biomaterials: design, testing, and best practice, Springer International Publishing, 2014.

[5] W.F. Ng, K.Y. Chiu and F.T. Cheng, Effect of pH on the in vitro corrosion rate of magnesium degradable implant material, Materials Science and Engineering: C (2010) 898-903.

[6] J. Kuhlmann, I. Bartsch, E. Willbold, S. Schuchardt, O. Holz, N. Hort, D. Höche, W.R. Heineman and F. Witte, Fast escape of hydrogen from gas cavities around corroding magnesium implants, Acta Biomaterialia 9 (2013) 8714-8721.

[7] M.P. Staiger, A.M. Pietak, J. Huadmai and G. Dias, Magnesium and its alloys as orthopedic biomaterials: a review, Biomaterials 27 (2006) 1728-1734.

[8] G. Song, Control of biodegradation of biocompatable magnesium alloys, Corrosion Science 49 (2007) 1696-1701.

[9] F. Witte, J. Fischer, J. Nellesen, H.A. Crostack, V. Kaese, A. Pisch, F. Beckmann and H. Windhagen, In vitro and in vivo corrosion measurements of magnesium alloys, Biomaterials 27 (2006) 1013-1018.

[10] F. Witte, F. Feyerabend, P. Maier, J. Fischer, M. Störmer, C. Blawert, W. Dietzel, N. Hort, Biodegradable magnesium-hydroxyapatite metal matrix composites, Biomaterials 28 (2007) 2163-2174.

[11] M.J. Shen, X.J. Wang, C.D Li, M.F. Zhang, X.S. Hu, M.Y. Zheng and K. Wu, Effect of bimodal size SiC particulates on microstructure and mechanical properties of AZ31B magnesium matrix composites, Materials and Design 52 (2013) 1011-1017.

[12] S. Tiwari, R. Balasubramaniam and M. Gupta, Corrosion behavior of SiC reinforced magnesium composites, Corrosion Science 49 (2007) 711-725.

[13] R. Relttig and S. Virtanen, Time-dependent electrochemical characterization of the corrosion of a magnesium rare-earth alloy in simulated body fluids, Journal of Biomedical Materials Research A85 A(2008)167-175

[14] DIN 50106, Testing of Metallic Materials; Compression Test (1978).

[15] ISO10993-5, Biological evaluation of medical devices - Part 5: Tests for cytotoxicity: In vitro methods, International Standards Organization, Geneva (1993).

[15] M.A. Azeem, A. Tewari, S. Mishra, S. Gollapudi, U. Ramamurty, Development of novel grain morphology during hot extrusion of magnesium AZ21 alloy, Acta Materialia 58 (2010) 1945-1502

[16] X. Wang, X. Hu, K. Nie, K. Wu, M. Zheng, Hot extrusion of SiC_p/AZ91 Mg matrix composites, Trans. Nonferrous Met. Soc. China 22 (2012) 1912-1917

[17] A. Feng and Y. Han, Mechanical and *in vitro* degradation behaviour of ultrafine calcium polyphosphate reinforced magnesium-alloy composites, Materials and Design 32 (2011) 2813-2820

[18] X. Gu, W. Zhou, Y. Zheng, L. Dong, Y. Xi, D. Chai, Microstructure, mechanical property, bio-corrosion and cytotoxicity evaluations of Mg/HA composites, Materials Science and Engineering C 30 (2010) 827-832